Heliyon 10 (2024) e27082

Contents lists available at ScienceDirect

Heliyon

journal homepage: www.cell.com/heliyon

Research article

Jianpi Jiedu decoction reverses 5-fluorouracil resistance in colorectal cancer by suppressing the xCT/GSH/GPX4 axis to induce ferroptosis

Qin-ling Ou [a,b], Lin Cheng [a], Yong-long Chang [a], Jin-hui Liu [c], Si-fang Zhang [a,b,*]

[a] *Department of Integrated Traditional Chinese & Western Medicine, The Second Xiangya Hospital, Central South University, Changsha, Hunan, 410011, China*

[b] *National Clinical Research Center for Metabolic Diseases, Changsha, Hunan, 410011, China*

[c] *College of Integrated Traditional Chinese & Western Medicine, Hunan University of Traditional Chinese Medicine, Changsha, Hunan, 410208, China*

ARTICLE INFO

Keywords:
Colorectal cancer
Jianpi Jiedu decoction
5-fluorouracil resistance
ferroptosis

ABSTRACT

Introduction: Innate and acquired chemoresistance in colorectal cancer (CRC) often results in 5-fluorouracil (5-FU) treatment failure. This study aimed to investigate the potential of Jianpi Jiedu (JPJD) decoction to reverse 5-FU resistance in CRC and clarify its potential mechanism of action.

Methods: The CCK-8 assay was employed to assess cell activity. Flow cytometry was employed to assess various parameters including cell apoptosis, cell cycle distribution, P-glycoprotein (P-gp) activity, reactive oxygen species levels, and lipid peroxidation. Metabolomics analysis was conducted to identify differentially expressed metabolites. Western blotting was utilized for protein expression analysis.

Results: In this study, we demonstrated that the combined JPJD and 5-FU treatment reversed 5-FU resistance in HCT8/5-FU cells, inducing cell apoptosis, causing G2/M-phase cell cycle arrest, and reducing P-gp protein expression and activity. Metabolomics analysis revealed ferroptosis as a key pathway in the development of 5-FU resistance. Furthermore, the combination treatment reversed drug resistance primarily by impacting ferroptosis and triggering critical ferroptosis events through the suppression of the cystine/glutamate transporter (xCT)/glutathione (GSH)/glutathione peroxidase (GPX4) axis.

Conclusion: JPJD decoction primarily suppressed the xCT/GSH/GPX4 axis to trigger ferroptosis, thereby effectively reversing 5-FU resistance in colorectal cancer (CRC).

1. Introduction

Colorectal cancer (CRC) ranks third among the most frequently diagnosed cancers and is the second leading cause of cancer-related deaths worldwide [1]. Despite advances in diagnosis and treatment, CRC remains highly lethal due to its resistance to treatments and propensity for metastasis. In total, 50%–60% of patients with CRC are diagnosed with colorectal metastases, necessitating neoadjuvant

* Corresponding author. Department of Integrated Traditional Chinese & Western Medicine, The Second Xiangya Hospital, Central South University, No.139 Middle Renmin Road, Changsha, Hunan 410011, China.

E-mail address: sifangzhang2005@csu.edu.cn (S.-f. Zhang).

https://doi.org/10.1016/j.heliyon.2024.e27082
Received 1 November 2023; Received in revised form 30 January 2024; Accepted 23 February 2024
Available online 25 February 2024

or adjuvant treatments alone or in combination with targeted therapies [2]. These treatments typically involve cytotoxic chemotherapeutic drugs, with 5-fluorouracil (5-FU) being the key agent for CRC treatment. However, genetic variations in tumor somatic cells leads to innate chemoresistance before therapy, while the genetic instability of malignant tumors contributes to acquired chemoresistance during therapy [3].

Approximately 90% of patients with metastatic cancer exhibit innate and acquired chemoresistance [4], resulting in tumor recurrence and progression, ultimately leading to 5-FU treatment failure. Therefore, there is an urgent need for innovative approaches to reverse 5-FU resistance in CRC.

Ferroptosis, a newly discovered type of cell death, sets itself apart from apoptosis, necrosis, and autophagy in terms of morphology and bioenergetics. The main characteristic of ferroptosis is the substantial accumulation of lethal lipid reactive oxygen species (ROS) in an iron-dependent manner [5].

Recent findings emphasize the potential of inducing ferroptosis as a cancer treatment strategy to overcome resistance to conventional therapies in aggressive malignancies while inhibiting ferroptosis promotes chemoresistance in CRC [6,7]. Ferroptosis is more likely to occur in therapy-resistant cancer cells that have undergone epithelial-mesenchymal transition compared to non-resistant cells [8]. Thus, inducing ferroptosis represents a promising therapeutic strategy to reverse chemoresistance.

Traditional Chinese medicine (TCM), with its unique theoretical system, diagnostic procedures, and treatments, has evolved over millennia in Asian nations, particularly China. As an adjuvant therapy for cancer, TCM can mitigate the side effects of chemotherapy, enhance patient immunity, improve patient quality of life, and augment the anti-tumor effect of conventional chemotherapy [9,10]. A meta-analysis demonstrated that associating TCM with capecitabine-based chemotherapy yielded greater anti-cancer efficacy compared to administering capecitabine monotherapy in CRC [11].

Therefore, considering TCM as a viable CRC treatment could be advantageous. Jianpi Jiedu decoction (JPJD), a clinically derived TCM formula, has been studied in CRC for years, exhibiting beneficial effects such as extended survival time and improved likelihood of survival in patients with stage II and III CRC [12]. Additionally, it significantly enhances treatment efficacy, reduces chemotherapy-related side effects, and ultimately improves the quality of life in patients with advanced CRC [13]. Furthermore, JPJD significantly inhibits CRC cell proliferation, migration, invasion, and angiogenesis and induces apoptosis through modulation of the mammalian target of rapamycin (mTOR)/hypoxia-inducible factor 1-alpha (HIF-1α)/vascular endothelial growth factor (VEGF) pathway [14]. These findings highlight the therapeutic potential of JPJD and its potential to reverse 5-FU resistance in CRC when used in combination therapy.

Herein, we investigated whether JPJD combined with 5-FU could reverse 5-FU resistance in CRC and elucidate the mechanism underlying the resistance reversal through metabolomics. We demonstrated that JPJD reversed 5-FU resistance by inducing ferroptosis in 5-FU-resistant CRC cells (HCT8/5-FU), downregulating cystine/glutamate transporter (xCT) and glutathione peroxidase 4 (GPX4) expression, and reducing glutathione (GSH) content. Furthermore, these cancer cells exhibited iron-dependent accumulation of lipid peroxidation products. Taken together, our findings provide new insights into TCM therapies against chemoresistance and contribute to the understanding of chemoresistance mechanisms.

2. Materials and methods

2.1. JPJD preparation

The herbal formula JPJD comprises eleven components in the following proportions: *Astragalus propinquus* Schischkin (20 g), Panax quinquefolius L. (10 g), Atractylodes macrocephala Koidz. (10 g), Poria cocos (Schw). Wolf (15 g), Coix aquatica Roxb. (20 g), Smilax aberrans Gagnep (20 g), Oldenlandia diffusa (Willd.) Roxb. (30 g), Scutellaria barbata D. Don (30 g), Paridis Rhizoma (10 g), Actinidia chinensis Planch. (20 g), and Glycyrrhiza uralensis Fisch. (5 g) in a ratio of 4:2:2:3:4:4:6:6:2:4:1. These herbs were procured from the Traditional Chinese Medicine Pharmacy of the Second Xiangya Hospital of Central South University, Hunan, China.

Following a standard preparation protocol, we derived a lyophilized powder of JPJD from crude water extracts of the blended herbs. Each gram of JPJD lyophilized powder was derived from 8.04 g of the original herbs mix and stored at −20 °C for subsequent use. These powders were dissolved in water to achieve a 10 mg/mL solution, which was then filtered through a 0.45 μm membrane.

2.2. Cell cultures

The human CRC cell line HCT8 was obtained from Procell Life Science & Technology Co., LTD (Wuhan, China). 5-FU-resistant CRC cell line HCT8/5-FU was obtained by exposing parental cells HCT8 to increasing concentrations of 5-FU for over 7 months, followed by testing to demonstrate resistance to 5-FU. All cell lines were cultured in RPMI 1640 medium, supplemented with 10% fetal bovine serum (FBS), 100 U/mL penicillin, and 100 μg/mL streptomycin all obtained from Gibco, USA. Moreover, HCT8/5-Fu cells specifically received 5 μg/ml 5-Fu (Sigma-Aldrich, St. Louis, MO, United States). Cultures were maintained at 37 °C within a humidified atmosphere composed of 95% air and 5% CO2.

2.3. Cytotoxic assay

HCT8 and HCT8/5-FU cells (5×10^3 cells/well) were incubated with varying concentrations of 5-FU (dissolved in water to make a 10 mg/mL solution) for 48 h. Cytotoxicity was assessed at 450 nm absorbance using the Cell Counting Kit-8 (CCK-8, Beyotime Biotechnology, Shanghai, China). The reversal index (RI) was calculated as.

RI═IC50 (HCT8/5-FU)/IC50 (HCT8) [15].with the half-maximal inhibitory concentration (IC50) value representing the concentration of 5-FU at which the cytotoxicity is reduced by half in HCT8 and HCT8/5-FU cells.

2.4. Cell viability assay

HCT8/5-FU cells (5×10^3 cells/well) were seeded in a 96-well plate and subsequently treated with varying concentrations of JPJD (0, 250, 500, 750, 1000, and 1250 μg/mL) for 48 h. Then, the absorbance was read at 450 nm using the CCK-8 assay. The 20% inhibitory concentration (IC_{20}) value was used to assess the maximum non-toxic concentration of the combination therapy.

2.5. Detection of reversing drug resistance

HCT8/5-FU cells (5×10^3 cells/well) were cultured in a 96-well plate and incubated overnight. Subsequently, the cells were co-treated with JPJD and 5-FU for 48 h. Cell viability was assessed using the CCK-8 assay and measuring the absorbance at 450 nm. The reversal fold (RF) in HCT8/5-FU cells was calculated as:

RF═IC50 (JPJD+5-FU group)/IC50 (5-FU group) [15].

2.6. Cell apoptosis and cycle analysis

HCT8/5-FU cells were cultured in 6-well plates (2×10^5 cells/well), treated with JPJD, 5-FU, and their combination for 48 h. Post incubation, cells were harvested and washed twice with phosphate-buffered saline (PBS). Apoptosis was evaluated using the Annexin V-FITC Apoptosis Detection Kit (Beyotime Biotechnology, Shanghai, China). The cells, after harvesting, were resuspended in 195 μL binding buffer, stained with 5 μL annexin V conjugated with fluorescein isothiocyanate and 10 μL propidium iodide (PI), and incubated at room temperature, shielded from light, for 15 min. Assessment of apoptosis was performed using a FACSCalibur Flow Cytometer (Becton Dickinson Co., Franklin Lakes, NJ, USA). Cell cycle analysis employed the Cell Cycle and Apoptosis Analysis Kit (Beyotime Biotechnology, Shanghai, China).

The cell harvesting and rinsing procedure followed the previously mentioned steps.

Subsequently, cells were incubated in pre-chilled 70% ethanol at 4 °C overnight, rinsed once with PBS the next day, and stained with PI solution for 30 min at 37 °C in the dark, following the manufacturer's instructions. Cell cycle analysis was conducted using the FACSCalibur Flow Cytometer, and data was utilized with FlowJo_v10.6.2.

2.7. Rhodamine 123 assay

Rhodamine 123 (#83702) was acquired from Sigma-Aldrich (Shanghai, China) to investigate the transporter activity of P-glycoprotein (P-gp). HCT8/5-FU cells were cultured in 6-well plates and exposed to JPJD, 5-FU, and their combination for 48 h. HCT8 cells were solely incubated with the medium. Subsequently, the cells were harvested, rinsed twice with PBS, resuspended in 1 mL of PBS, and incubated with 5 μM rhodamine 123 and 37 °C for 30 min. Cell properties were determined using a flow cytometer equipped with a 507 nm laser, and data were evaluated using FlowJo_v10.6.2.

2.8. Measurement of ROS assay

The Reactive Oxygen Species Assay Kit (#S0033) was obtained from Beyotime Biotechnology. Cells were cultured in 6-well plates and subjected to the same treatment as previously outlined. Following the manufacturer's instructions, cells were incubated with dichlorodihydrofluorescein diacetate (DCFH-DA; 10 μM) at 37 °C for 20 min with intermittent mixing. Subsequently, cells were thrice rinsed with serum-free medium and analyzed via flow cytometry to assess intracellular ROS levels.

2.9. Glutathione (GSH) assay

The Total Glutathione Assay Kit (#S0052; Beyotime Biotechnology) was used to quantify total GSH, according to the manufacturer's instructions. Sample detection was performed with a Microplate Reader (Thermo Fisher Scientific Co., Ltd) set at a wavelength of 412 nm.

2.10. Lipid ROS assay

The BODIPY 581/591 C11(D3861, Thermo Fisher Scientific) reagent was used to measure the intracellular lipid ROS levels. Cells were initially seeded in 6-well plates incubated for 24 h. Subsequently, HCT8/5-FU cells were treated with JPJD, 5-FU, or their association (with or without ferrostatin-1 [Fer-1] or liproxstatin-1 [Lip-1]) for 48 h. Fer-1 (5 μM) and Lip-1 (5 μM) were added to the corresponding groups, and the mixtures were incubated for 2 h. After harvest, cells were washed twice, resuspended in 500 μL of PBS, and stained with 2 μM BODIPY 581/591 C11 reagent at 37 °C for 30 min. After a single wash with PBS, cells were detected using a flow cytometer. Data were analyzed by FlowJo_v10.6.2.

2.11. Cellular iron assay

To assess cellular iron, FerroOrange (#F374, Dojindo Molecular Technologies Inc.) was employed. Cells were initially seeded in 96-well plates (5×10^3 cells/well) for 24 h,followed by treatment with JPJD, 5-FU, and their association (with or without Fer-1 or Lip-1) for 48 h. After two PBS washes, cells were stained with 10 μg/mL DAPI for 10 min, followed by two additional washes with FBS-free medium. Subsequently, cells were stained with 0.2 μM FerroOrange for 10 min and examined using an inverted fluorescent microscope (Thermo Fisher Scientific Co., Ltd).

2.12. Western blot analysis

Antibodies targeting xCT and GPX4 were procured from Abcam, whereas Bcl-2-associated X protein (BAX), B-cell lymphoma 2 (Bcl-2), poly (ADP-ribose) polymerase family member 1(PARP1), Cyclin B1, Cyclin D1 and P-gp were sourced from Proteintech. Cells were harvested and lysed using a Radioimmunoprecipitation Assay buffer (Beyotime, Shanghai, China). Protein quantification was conducted with a BCA Protein Assay Kit. Subsequently, the lysates were loaded onto a 5–20% Tris-Tricine Ready Gel for sodium dodecyl-sulfate polyacrylamide gel electrophoresis, followed by blotting onto a nitrocellulose membrane. The membranes were blocked with 5% skim milk for 1 h before exposure to primary antibodies. Subsequently, immunoreactive bands were incubated with secondary antibodies of horseradish-peroxidase-conjugated and visualized with a chemiluminescence detection system (Thermo Fisher Scientific Co., Ltd).

2.13. Metabolomics analysis

Metabolomic analyses were undertaken by Majorbio Bio-Pharm Technology Co. Ltd. (Shanghai, China). Metabolite profiling was conducted utilizing several sample groups including the control group (HCT8/5-FU cells alone, n = 6), JPJD group (HCT8/5-FU cells treated with 450 μg/mL JPJD, n = 6), JPJD+5-FU group (HCT8/5-FU cells treated with 450 μg/mL JPJD and 150 μg/ml 5-FU, n = 6) and HCT8 group (HCT8 cells alone, n = 6).

Liquid chromatography-tandem mass spectrometry (MS) analysis was performed using a Thermo UHPLC-Q Exactive HF-X system, featuring an ACQUITY HSS T3 column (100 mm × 2.1 mm i.d., 1.8 μm; Waters, USA). The mobile phases included 0.1% formic acid in water: acetonitrile (95:5, v/v) (solvent A) and 0.1% formic acid in acetonitrile: isopropanol: water (47.5:47.5, v/v) (solvent B).

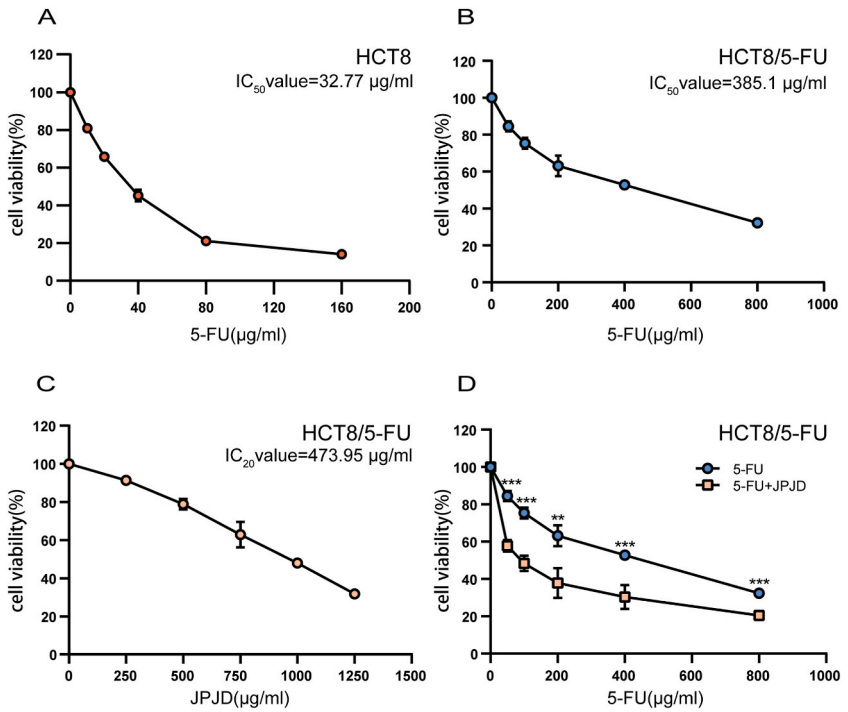

Fig. 1. Combination treatment of Jianpi Jiedu (JPJD) and 5-fluorouracil (5-FU) reversed 5-FU resistance in HCT8/5-FU cells
(A) The 50% inhibitory concentration (IC_{50}) value of 5-FU in HCT8 cells (32.77 μg/mL) and **(B)** HCT8/5-FU cells (385.1 μg/mL) after 48 h of treatment, detected using the CCK-8 assay. (**C**) The 20% inhibitory concentration (IC_{20}) value of JPJD (473.95 μg/mL) in HCT8/5-FU cells after 48 h of treatment. (**D**) JPJD (450 μg/mL) was combined with varying concentrations of 5-FU (ranging from 0 to 800 μg/mL) for 48 h. HCT8/5-FU cells were exposed to the combination therapy to evaluate its inhibitory effect and cytotoxicity compared to 5-FU alone. Data are expressed as the mean ± standard deviation; $^{**}P < 0.01$, $^{***}P < 0.001$.

Maintaining a flow rate of 0.40 mL/min at 40 °C column temperature, mass spectrometric data were collected using a Thermo UHPLC-Q Exactive HF-X Mass Spectrometer. The instrument was equipped with an electrospray ionization source operating in both positive and negative modes.

Setting optimal conditions, the following parameters were established: a source temperature of 425 °C, a sheath gas flow rate of 50 arb, an auxiliary gas flow rate of 13 arb, and an ion-spray voltage floating set at −3500 V in negative mode and 3500 V in positive mode. MS/MS utilized a normalized collision energy ranging from 20 to 60 V, with full MS resolution set at 60000 and MS/MS resolution at 7500.

In Data Dependent Acquisition (DDA) mode, data acquisition covered a mass range of 70–1050 *m/z*. Principal Component Analysis (PCA) ensured quality control during initial data analysis. Discrimination Analysis, including Partial Least Squares Discrimination Analysis (PLS-DA) and Orthogonal PLS-DA, revealed group differences. Differential metabolites were identified based on variable

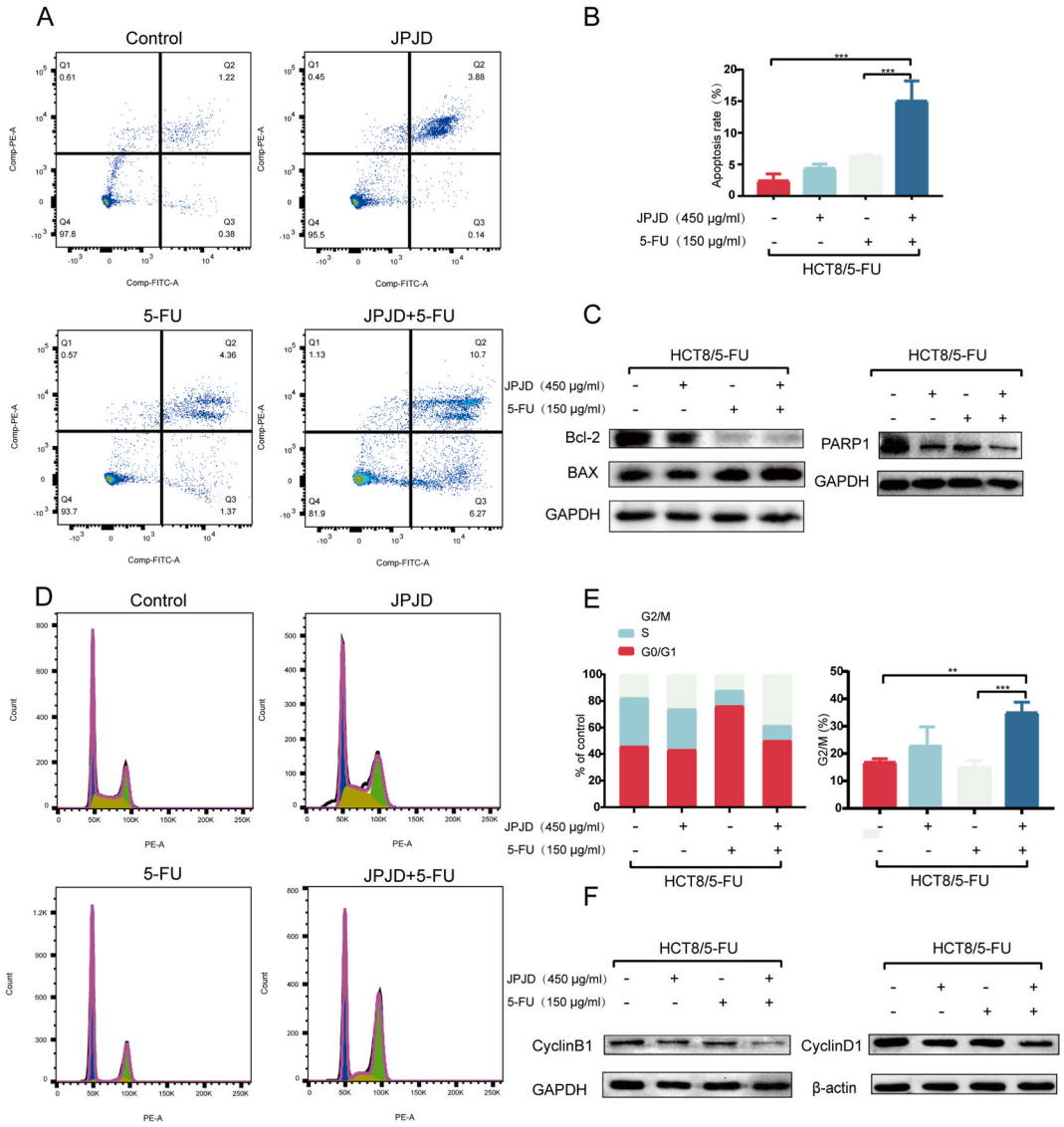

Fig. 2. Combination treatment of Jianpi Jiedu (JPJD) and 5-fluorouracil (5-FU) induced cell apoptosis and cell cycle arrest
(A) Representative results of annexin V-fluorescein isothiocyanate/propidium iodide (PI) staining and **(B)** quantitative analysis after exposure of HCT8/5-FU cells to the treatment (JPJD 450 μg/mL+ 5-FU 150 μg/mL or 5-FU/JPJD monotherapy) for 48 h. **(C)** The expression of Bcl-2, BAX and PARP1 in HCT8/5-FU cells after exposure to the treatment (JPJD 450 μg/mL + 5-FU 150 μg/mL or 5-FU/JPJD monotherapy) for 48 h, detected using Western blotting. (**D**) Representative results of PI staining, (**E**) quantitative analysis and the proportion of cells in the G2/M phase after exposure of HCT8/5-FU cells to the treatment (JPJD 450 μg/mL + 5-FU 150 μg/mL or 5-FU/JPJD monotherapy) for 48 h. (**F**) The expression of CyclinB1 and CyclinD1 in HCT8/5-FU cells after exposure to the treatment (JPJD 450 μg/mL + 5-FU 150 μg/mL or 5-FU/JPJD monotherapy) for 48 h, detected using Western blotting. Original images of Western blot are uploaded as supplementary material S6 A-B. Data are expressed as mean ± standard deviation, **P < 0.01, ***P < 0.001.

importance (VIP) > 1 and P-value <0.05. Advanced analyses, such as heatmap and Kyoto Encyclopedia of Genes and Genomes (KEGG) enrichment, were performed using the Majorbio Cloud Platform.

2.14. Statistical analysis

Presented as mean ± standard deviation from three repetitions, the results were analyzed using GraphPad Prism Software (Version Prism 8; GraphPad Software, Inc.). A Student's t-test was employed to differentiate results between two groups, and a one-way ANOVA was utilized for comparisons amongst multiple groups. Statistical significance was defined as a p-value <0.05.

3. Results

3.1. JPJD and 5-FU combined treatment reverses 5-FU resistance in HCT8/5-FU cells

Initially, drug resistance was confirmed in HCT8/5-FU cells. Cell viability was assessed using the CCK-8 assay, revealing an IC50 value of 32.77 μg/mL for 5-FU and parental HCT8 cells (Fig. 1A), and of 385.1 μg/mL for HCT8/5-FU cells (Fig. 1B). This 11.8-fold difference confirmed the resistance of HCT8/5-FU cells to 5-FU. The impact of JPJD on HCT8/5-FU cells was examined using CCK-8 assays, employing concentrations ranging from 0 to 1250 μg/mL administered over 48 h. The maximum non-toxic concentration, IC20, was 473.95 μg/mL (Fig. 1C). Subsequently, a combination of JPJD (450 μg/mL) and various concentrations of 5-FU ranging from 0 to 800 μg/mL was administered for 48 h to evaluate the inhibitory effect and cytotoxicity of the combination treatment.

The combination of JPJD with 5-FU significantly reduced the viability of HCT8/5-FU cells compared to 5-FU alone (Fig. 1D). In the combination group, the IC50 value of 5-FU was 87.63 μg/mL, with an RI 4.39-fold higher than that of the 5-FU group. These findings confirmed that JPJD can reverse 5-FU resistance in HCT8/5-FU cells. Subsequent experiments utilized HCT8/5-FU cells treated with 450 μg/mL JPJD and 150 μg/mL 5-FU (approximately half the IC50 value) for 48 h.

3.2. Combining JPJD and 5-FU induced apoptosis and cell cycle arrest

Flow cytometry was used to accurately assess the impact of treatment on apoptosis and cell death in HCT8/5-FU cells. Cells were grouped based on the corresponding treatment and stained with annexin V-FITC and PI. The assay revealed a significant increase in the percentage of apoptotic cells with the 5-FU and JPJD combination (Fig. 2A–B). Western blot analysis demonstrated significantly higher levels of BAX expression and lower levels of Bcl-2 and PARP1 expression in the combination treatment group compared to the control group (Fig. 2C and S1 A-C), with the former exhibiting an elevated BAX/Bcl-2 ratio, indicating that the combination therapy induced apoptosis.

To investigate whether treatment-induced growth inhibition correlated with cell cycle arrest, the cell cycle distribution was assessed using flow cytometric analysis. The combination of 5-FU and JPJD induced cell cycle arrest at the G2/M phase (Fig. 2D–E). Western blot analysis showed significantly lower levels of Cyclin B1 and Cyclin D1 expression in the combination treatment group compared to the control group (Fig. 2F and S1 D-E), and it is consistent with the flow cytometric results.

In summary, these results demonstrate that the combination treatment of 5-FU and JPJD effectively sensitizes HCT8/5-FU cells by inducing cell apoptosis and G2/M-phase arrest.

3.3. Combining JPJD with 5-FU reduced the expression of P-gp and suppressed its activity

P-gp, an ATP-binding cassette (ABC) membrane transporter, acts as a drug efflux pump, and its high expression was detected in drug-resistant cancer cells. P-gp confers resistance to various anti-cancer drugs by reducing intracellular drug concentration [16]. To

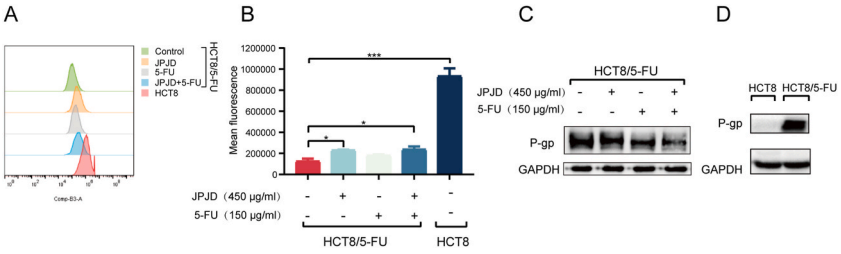

Fig. 3. Combination treatment of Jianpi Jiedu (JPJD) and 5-fluorouracil (5-FU) suppressed the expression of P-glycoprotein (P-gp) and inhibited its activity

(**A**) Representative results of Rhodamine 123 staining and (**B**) quantitative analysis after HCT8/5-FU cells exposure to the treatment (JPJD 450 μg/mL + 5-FU 150 μg/mL or 5-FU/JPJD monotherapy) and HCT8 cells for 48 h. (**C**) The expression of P-gp in HCT8/5-FU cells after exposure to the treatment (JPJD 450 μg/mL + 5-FU 150 μg/mL or 5-FU/JPJD monotherapy) for 48 h. (D) The expression of P-gp between HCT8 and HCT8/5-FU cells. Original images of Western blot are uploaded as supplementary material S6 C-D. Data are expressed as mean ± standard deviation, *P < 0.05, ***P < 0.001.

investigate whether JPJD reverses 5-FU resistance by suppressing P-gp, HCT8 and HCT8/5-FU cells (exposed to the corresponding treatments) were stained with rhodamine 123, a fluorescent dye transported by P-gp, and analyzed by flow cytometry [17]. Compared to the HCT8 group, the control group exhibited a significantly left-shifted peak figure, and a substantially lower mean fluorescence intensity (MFI).Compared to the control group, the peak figure in JPJD and JPJD+5-FU groups shifted significantly to the right, with a noticeable increase in cell MFI. These results indicated a significant increase in P-gp drug efflux activity during the transition from

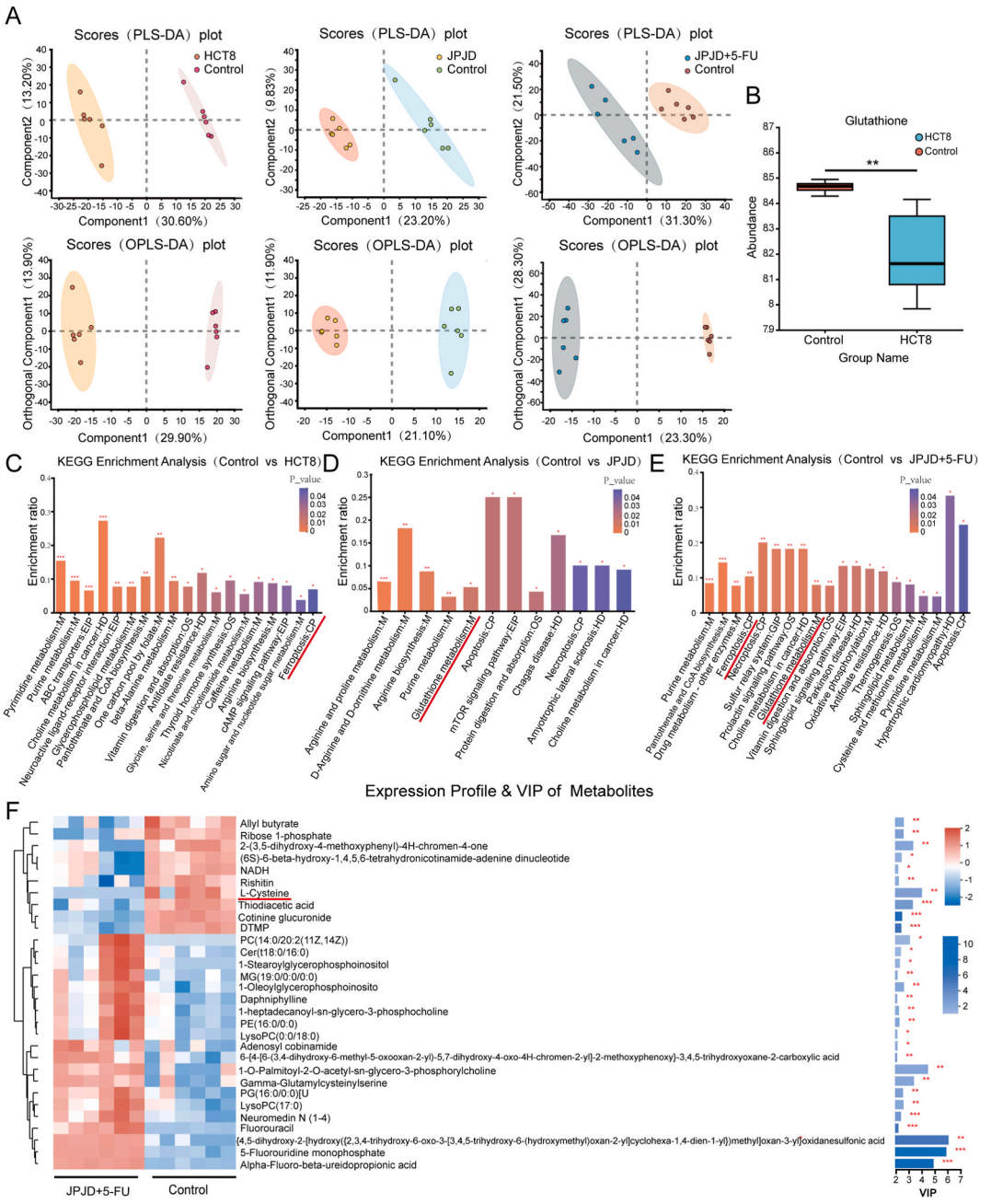

Fig. 4. Differential metabolites were identified between the control group and the HCT8 or Jianpi Jiedu (JPJD) or JPJD+5-fluorouracil (5-FU) group

(A) Discrimination and orthogonal partial least squares discrimination analyses models assessing differences between the control group (HCT8/5-FU cells alone) vs. HCT8 group, control group vs. JPJD group, and control group vs. JPJD+5-FU group. (**B**) Glutathione levels detected using metabolomics in control vs HCT8 group. The Kyoto Encyclopedia of Genes and Genomes enrichment analysis in the control group vs. HCT8 group (C), control group vs. JPJD group, (D) and control group vs. JPJD+5-FU group (E). Heat map illustrating the differences between the control group vs. JPJD+5-FU group (F). Data are expressed as mean ± standard deviation. $^{**}P < 0.01$.

HCT8 to HCT8/5-FU cells, and JPJD effectively reversed 5-FU resistance in HCT8/5-FU cells by suppressing this activity (Fig. 3A–B).

The expression level of P-gp was significantly lower in the cells treated with the combination treatment compared to control group (Fig. 3C and S1F). Moreover, the expression level of P-gp was significantly higher in the HCT8/5-FU cells compared to HCT8 cells (Fig. 3D and S1G).

These findings suggest that JPJD inhibits the activity and reduces the expression of P-gp, enhancing the efficacy of 5-FU.

3.4. The metabolomics analysis revealed alterations in the metabolic profile induced by JPJD and combination treatment

PLS-DA and OPLS-DA highlighted significant distinctions between the control group and the HCT8, JPJD, and JPJD+5-FU groups (Fig. 4A). Specifically, 138 metabolites exhibited significant alterations between the control group and the HCT8 group. Similarly, 95 and 94 metabolites displayed significant modifications between the control group and the JPJD group or the JPJD+5-FU group, respectively (Fig. S2).

Subsequent KEGG enrichment analysis revealed 19 pathways exhibiting significant differences between the control group and the HCT8 group. Notably, ABC transporters and ferroptosis were associated with drug resistance (Fig. 4C). Moreover, compared to the HCT8 group, the control group demonstrated a significant increase in GSH, a key metabolite implicated in ferroptosis (Fig. 4B).

Additionally, KEGG enrichment analysis disclosed 12 predominantly altered pathways between the control and JPJD groups, encompassing glutathione metabolism, apoptosis, the mTOR signaling pathway, and necroptosis, all related to drug resistance (Fig. 4D). KEGG enrichment analysis further revealed that 20 drug resistance-related pathways including ferroptosis, necroptosis, glutathione metabolism, and apoptosis were significantly altered between the control and JPJD+5-FU groups (Fig. 4E). Furthermore, a heat map comparing the control and JPJD+5-FU groups revealed the top thirty significantly differentially expressed metabolites (Fig. 4F). Compared to the control group, all samples in the JPJD+5-FU group exhibited a significant decrease in the intracellular content of L-cysteine, a crucial substrate for GSH biosynthesis. Therefore, we hypothesized that the combination of JPJD and 5-FU may impact GSH biosynthesis via L-cysteine, thereby inducing ferroptosis and reversing 5-FU resistance in HCT8/5-FU cells.

3.5. Combining JPJD and 5-FU decreased intracellular GSH content and the expression level of xCT

We investigated the role of GSH in the reversal of 5-FU resistance by JPJD. The combination treatment significantly reduced GSH levels compared to the monotherapy (Fig. 5A), indicating that the former induced GSH depletion and might impact GSH biosynthesis.

The transmembrane protein complex system xc−, consisting of subunits xCT (also known as SLC7A11) and SLC3A2, acts as a cystine/glutamate antiporter to import cystine. In cells, cystine is reduced to cysteine, a rate-limiting substrate for GSH biosynthesis. xCT plays a crucial role in the activity of the system xc− and determines the intracellular cystine content [18]. Metabolomics indicated that the combination treatment reduced the intracellular content of L-cysteine compared to 5-FU monotherapy. To validate the efficacy of the combined therapy on xCT, Western blotting and ELISA were employed to measure its expression level. Both assays demonstrated a significant reduction in xCT expression with the combined treatment (Fig. 5B–C and S1H). Overall, these findings indicate that the combination treatment leads to a reduction in xCT expression and suppression of GSH biosynthesis.

3.6. Combining JPJD and 5-FU induced ferroptosis in HCT8/5-FU cells

Considering the previous results, we further hypothesized that the combined treatment may induce ferroptosis, reversing 5-FU resistance in HCT8/5-FU cells. The expression of GPX4, a reductase that mitigates lipid peroxide accumulation and inhibits ferroptosis, exhibited a significant decrease in the combined therapy group compared to the 5-FU group (Fig. 6A and S1I), as confirmed by Western blot analysis. We further assessed several key ferroptosis processes in HCT8/5-FU cells exposed to the combination treatment, including the levels of ROS, lipid peroxidation, and intracellular ferrous ions (GSH depletion was already determined).

Intracellular ROS content, measured by the DCFH–DA fluorescent probe sensitive to ROS, significantly increased with the

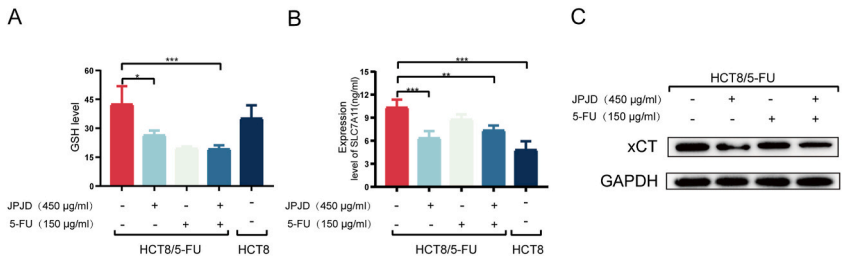

Fig. 5. Combination treatment of Jianpi Jiedu (JPJD) and 5-fluorouracil (5-FU) decreased the level of glutathione (GSH) and suppressed the expression of xCT

(A) Intracellular GSH levels in HCT8/5-FU cells after exposure to the treatment (JPJD 450 μg/mL + 5-FU 150 μg/mL or 5-FU/JPJD monotherapy) and HCT8 cells for 48 h. The expression of xCT in HCT8/5-FU cells after exposure to the treatment (JPJD 450 μg/mL + 5-FU 150 μg/mL or 5-FU/JPJD monotherapy) and HCT8 cells for 48 h, assessed using **(B)** ELISA and **(C)** Western blot. Original images of Western blot are uploaded as supplementary material S6 E. Data are expressed as the mean ± standard deviation; *P < 0.05, **P < 0.01, ***P < 0.001.

combination of 5-FU and JPJD compared to the control (Fig. 6B–C). Additionally, the combination treatment significantly increased lipid ROS, mirroring the trend observed for ROS (Fig. 6D–E).

We measured the intracellular ferrous ion levels using FerroOrange as iron is a critical reactive component in ferroptosis. The percentage of FerroOrange-positive cells in HCT8/5-FU cells increased with the combination therapy compared to the control, indicating the involvement of ferroptosis (Fig. 6F). Further, in HCT8/5-FU cells treated with the combination of 5-FU and JPJD, additional treatment with Lip-1 or Fer-1 resulted in a complete blockade of lipid ROS and ferrous ion accumulation, confirming the inhibitory effect of ferroptosis inhibitors (Fig. 6D–F).

Collectively, our findings demonstrate that the combination therapy significantly increases the accumulation of ROS, lipid ROS, and intracellular ferrous ion while reducing GPX4 expression levels, thereby inducing ferroptosis - a potential mechanism to reverse 5-FU resistance.

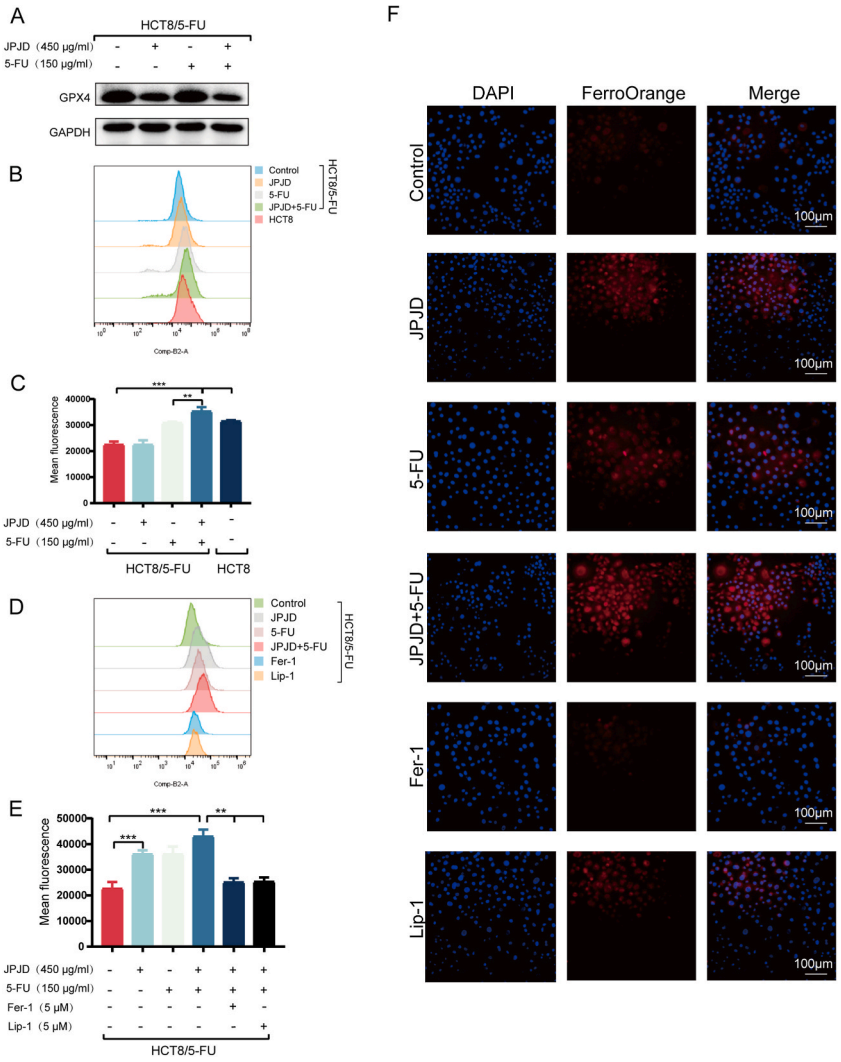

Fig. 6. Combination treatment of Jianpi Jiedu (JPJD) and 5-fluorouracil (5-FU) induced events characteristic for ferroptosis
(A)The expression of glutathione peroxidase 4 (GPX4) was detected after exposure of HCT8/5-FU cells to the treatment (JPJD 450 μg/mL + 5-FU 150 μg/mL or 5-FU monotherapy) for 48 h. (B) Cellular reactive oxygen species (ROS) levels and (C) quantitative analysis after exposure of HCT8/5-FU to the treatment (JPJD 450 μg/mL + 5-FU 150 μg/mL or 5-FU/JPJD monotherapy) and HCT8 cells for 48 h. (D) Cellular ROS lipid levels and quantitative analysis (E) after exposure of HCT8/5-FU cells to the treatment (JPJD 450 μg/mL + 5-FU 150 μg/mL with or without lip-1 and fer-1 or 5-FU/JPJD monotherapy) for 48 h. (F) Cellular ferrous ion content after exposure of HCT8/5-FU cells to the treatment (JPJD 450 μg/mL + 5-FU 150 μg/mL, with or without lip-1 and fer-1 or 5-FU/JPJD monotherapy) for 48 h, detected by fluorescence microscope. Original images of Western blot are uploaded as supplementary material S6 F. Data are expressed as mean ± standard deviation, $^{**}P < 0.01$, $^{***}P < 0.001$.

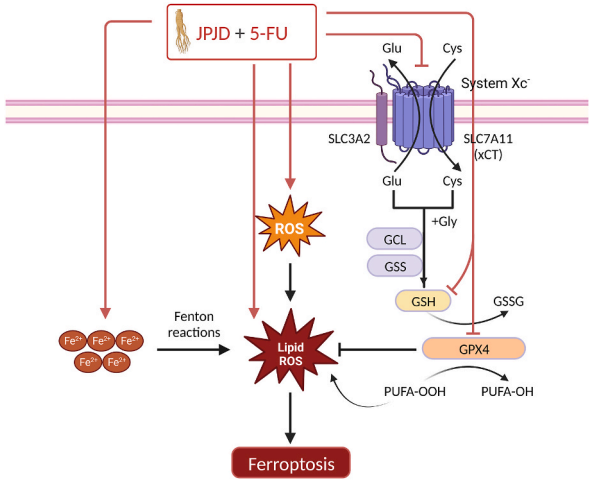

Fig. 7. A schematic diagram about the central role of Combination treatment of Jianpi Jiedu (JPJD) and 5-fluorouracil (5-FU) induced ferroptosis

The combination treatment of JPJD and 5-FU downregulates the expression of GPX4 and xCT, reduces GSH content, and increases ROS, lipid ROS, and iron levels, thereby inducing ferroptosis.

4. Discussion

As an adjunctive therapy in cancer treatment, TCM enhanced drug sensitivity, effectively suppressed tumors, improved patients' quality of life, and mitigated chemotherapy-related adverse reactions [19–21]. Numerous studies have investigated the efficacy of TCM in the treatment of CRC. For example, curcumin reversed chemotherapy resistance to 5-FU in CRC cells by reducing the proportion of cancer stem cells (CSC) [22]. Sijunzi decoction modulated the phosphoinositide 3-kinase/protein kinase B/mTOR pathway, leading to apoptosis and autophagy in CRC cells [23].

JPJD formula has shown anti-metastatic effects in CRC by downregulating integrin beta-like 1 (ITGBL1)-rich extracellular vesicle secretion and inhibiting fibroblast activation through the modulation of the ITGBL1/tumor necrosis factor alpha-induced protein 3/nuclear factor-κB signaling pathway [24]. Moreover, we have previously demonstrated the efficacy of JPJD decoction in inhibiting CRC cell proliferation and inducing apoptosis in HCT116 cells. Furthermore, JPJD exhibited notable anti-metastatic, anti-invasive, and anti-angiogenic properties through the regulation of the mTOR/HIF-1α/VEGF pathway [14]. These findings collectively indicate the potent anti-cancer properties of JPJD showcasing its effectiveness across multiple dimensions.

Chemotherapy resistance in CRC leads to the failure of 5-FU treatment, resulting in tumor recurrence and metastasis. Based on our previous findings [14], we hypothesized that JPJD has the potential to reverse 5-FU resistance in CRC, enhancing chemotherapy sensitivity. Herein, the CCK-8 assay confirmed our hypothesis, demonstrating that the combination of JPJD and 5-FU effectively reverses drug resistance in HCT8/5-FU cells. Simultaneously, JPJD induced cell apoptosis, arrested the cell cycle, inhibited P-gp activity and expression, and induced ferroptosis in HCT8/5-FU cells. This indicates that the reversal of drug resistance by JPJD involves a combination of multiple mechanisms and functions.

JPJD decoction, a TCM compound comprising 11 herbs, is characterized by its multi-component, multi-targeted, and multi-pathway nature. This complexity presents a challenge to understanding its comprehensive effects through conventional experimental methods. Metabolomics comprehensively analyzes the qualitative and quantitative profiles of low molecular weight metabolites in an organism or cell during a specific physiological period. Metabolomics, a crucial component of systems biology, aligns with the holistic perspective of TCM theory due to its unique dynamic viewpoint [25]. Therefore, we employed metabolomics to perform a thorough analysis of JPJD decoction effects. The drug-resistant HCT8/5-FU cells exhibited a significant increase in GSH content compared to HCT8 cells, suggesting an enhanced capacity to withstand oxidative stress. Furthermore, KEGG enrichment analysis indicated that both the transition from primitive cells to 5-FU-resistant cells and the primary function of combination therapy were associated with ferroptosis. Additionally, the combined therapy group exhibited a significant reduction in intracellular L-cysteine content compared to the control group. These findings suggest that inhibiting ferroptosis is pivotal in drug resistance development while inducing ferroptosis emerges as a promising strategy for its reversal.

Ferroptosis, a recently identified form of regulated cell death, is characterized by the iron-dependent accumulation of lipid peroxidation products, leading to plasma membrane rupture. Coined in 2012, the term 'ferroptosis' has spurred extensive research in various fields, including tumor therapy, ischemia-reperfusion injury, and Alzheimer's disease [26]. Emerging research has indicated a correlation between ferroptosis and drug resistance in cancer therapy, encompassing chemotherapy, immunotherapy, and targeted therapy [27]. Studies have reported that exosomes released by adipose tissue hinder the generation of lipid ROS, decrease cell susceptibility to ferroptosis, and promote chemotherapy resistance in CRC cells [7]. Additionally, the secretion of miR-522 by cancer-associated fibroblasts suppresses ALOX15 expression and diminishes lipid-ROS accumulation in cancer cells, inhibiting ferroptosis and reducing chemosensitivity [28]. GPX4 is a crucial enzyme in mammals, converting phospholipid hydroperoxides into

phospholipid alcohols, reducing lipid peroxidation accumulation, and inhibiting ferroptosis. Suppression of GPX4 induces ferroptosis and reverses drug sensitivity. Furthermore, inhibition of the kinesin family member 20A/NUAK family SNF1-like kinase 1/protein phosphatase 1 beta/GPX4 pathway effectively reverses oxaliplatin resistance in CRC cells [29].

Additionally, GSH, a GPX4 substrate, is essential in combating ferroptosis. The xc-system regulates cystine uptake, mediating GSH biosynthesis and suppressing ferroptosis [30]. Similarly, inhibiting xCT enhances ferroptosis susceptibility, overcoming drug resistance. Disruption of the nuclear factor-erythroid 2/Kelch-like ECH-associated protein 1/xCT signaling induced ferroptosis, rendering cisplatin-resistant gastric cancer cells more susceptible to cisplatin [31]. Our findings suggest that the combination therapy effectively reduces the expression levels of xCT and GPX4, resulting in decreased GSH content and increased lipid ROS and iron accumulation. These pivotal ferroptosis events were triggered by the combination treatment. Thus, we posit that JPJD primarily reverses 5-FU resistance in HCT8/5-FU cells by inducing ferroptosis.

5. Conclusions

Herein, employing a metabolomics-driven approach, we confirm for the first time that JPJD reverses 5-FU resistance in CRC cells, enhancing the anticancer effect of 5-FU. Moreover, the combination treatment of JPJD and 5-FU induces apoptosis, cell cycle arrest, suppresses the expression and activity of P-gp, downregulates the expression of GPX4 and xCT, reduces GSH content, and increases ROS, lipid ROS, and iron levels, thereby inducing ferroptosis. Thus, JPJD inhibits the xCT/GSH/GPX4 axis, triggering ferroptosis and reversing 5-FU resistance in CRC.

Data availability statement

Data will be made available on request.

Funding

This work was supported by the Research projects of traditional Chinese medicine of Hunan Province (No. A2023043), Hunan Provincial Health and Family Planning Commission Research Project (No. 20200424), Natural Science Foundation of Changsha (No. 2022467) and Hunan Provincial Clinical Medical Research Center Project (No. 2023SK4048)

Ethics approval statement

Not applicable.

CRediT authorship contribution statement

Qin-ling Ou: Visualization. **Lin Cheng:** Validation. **Yong-long Chang:** Software. **Jin-hui Liu:** Data curation. **Si-fang Zhang:** Conceptualization.

Declaration of competing interest

The authors declare that they have no known competing financial interests or personal relationships that could have appeared to influence the work reported in this paper.

Acknowledgments

We would like to acknowledge the convenience of BioRender (https://www.biorender.com/) for scientific mapping. And Fig. 7 was created with BioRender.com. We thank Bullet Edits Limited for the linguistic editing and proofreading of the manuscript.

Appendix A. Supplementary data

Supplementary data to this article can be found online at https://doi.org/10.1016/j.heliyon.2024.e27082.

References

[1] H. Sung, J. Ferlay, R.L. Siegel, M. Laversanne, I. Soerjomataram, A. Jemal, F. Bray, Global cancer statistics 2020: GLOBOCAN estimates of incidence and mortality worldwide for 36 cancers in 185 countries, CA A Cancer J. Clin. 71 (2021) 209–249, https://doi.org/10.3322/caac.21660.

[2] A.B. Benson, A.P. Venook, M.M. Al-Hawary, M.A. Arain, Y.-J. Chen, K.K. Ciombor, S. Cohen, H.S. Cooper, D. Deming, L. Farkas, I. Garrido-Laguna, J.L. Grem, A. Gunn, J.R. Hecht, S. Hoffe, J. Hubbard, S. Hunt, K.L. Johung, N. Kirilcuk, S. Krishnamurthi, W.A. Messersmith, J. Meyerhardt, E.D. Miller, M.F. Mulcahy, S. Nurkin, M.J. Overman, A. Parikh, H. Patel, K. Pedersen, L. Saltz, C. Schneider, D. Shibata, J.M. Skibber, C.T. Sofocleous, E.M. Stoffel, E. Stotsky-Himelfarb, C.

G. Willett, K.M. Gregory, L.A. Gurski, Colon cancer, version 2.2021, NCCN clinical practice guidelines in oncology, J. Natl. Compr. Cancer Netw. 19 (2021) 329–359, https://doi.org/10.6004/jnccn.2021.0012.
[3] W.A. Hammond, A. Swaika, K. Mody, Pharmacologic resistance in colorectal cancer: a review, Ther Adv Med Oncol 8 (2015) 57–84, https://doi.org/10.1177/1758834015614530.
[4] D. Longley, P. Johnston, Molecular mechanisms of drug resistance, J. Pathol. 205 (2005) 275–292, https://doi.org/10.1002/path.1706.
[5] S.J. Dixon, K.M. Lemberg, M.R. Lamprecht, R. Skouta, E.M. Zaitsev, C.E. Gleason, D.N. Patel, A.J. Bauer, A.M. Cantley, W.S. Yang, B. Morrison, B.R. Stockwell, Ferroptosis: an iron-dependent form of nonapoptotic cell death, Cell 149 (2012) 1060–1072, https://doi.org/10.1016/j.cell.2012.03.042.
[6] T. Zhu, L. Shi, C. Yu, Y. Dong, F. Qiu, L. Shen, Q. Qian, G. Zhou, X. Zhu, Ferroptosis promotes photodynamic therapy: supramolecular photosensitizer-inducer nanodrug for enhanced cancer treatment, Theranostics 9 (2019) 3293–3307, https://doi.org/10.7150/thno.32867.
[7] Q. Zhang, T. Deng, H. Zhang, D. Zuo, Q. Zhu, M. Bai, R. Liu, T. Ning, L. Zhang, Z. Yu, H. Zhang, Y. Ba, Adipocyte-derived exosomal MTTP suppresses ferroptosis and promotes chemoresistance in colorectal cancer, Adv. Sci. 9 (2022) 2203357, https://doi.org/10.1002/advs.202203357.
[8] M. Sang, R. Luo, Y. Bai, J. Dou, Z. Zhang, F. Liu, F. Feng, J. Xu, W. Liu, Mitochondrial membrane anchored photosensitive nano-device for lipid hydroperoxides burst and inducing ferroptosis to surmount therapy-resistant cancer, Theranostics 9 (2019) 6209–6223, https://doi.org/10.7150/thno.36283.
[9] Y. Wang, Q. Zhang, Y. Chen, C.-L. Liang, H. Liu, F. Qiu, Z. Dai, Antitumor effects of immunity-enhancing traditional Chinese medicine, Biomed. Pharmacother. 121 (2020) 109570, https://doi.org/10.1016/j.biopha.2019.109570.
[10] F. Qi, L. Zhao, A. Zhou, B. Zhang, A. Li, Z. Wang, J. Han, The advantages of using traditional Chinese medicine as an adjunctive therapy in the whole course of cancer treatment instead of only terminal stage of cancer, BST 9 (2015) 16–34, https://doi.org/10.5582/bst.2015.01019.
[11] H. Jiang, Y. Jiang, B. Yang, F. Long, Z. Yang, D. Tang, Traditional Chinese medicines and capecitabine-based chemotherapy for colorectal cancer treatment: a meta-analysis, Cancer Med. 12 (2022) 236–255, https://doi.org/10.1002/cam4.4896.
[12] F. Lin, L. Tian, C. Lei, C. Ding, L. Shi, S. Zhang, Chinese medicine for outcomes in colorectal cancer patients: a retrospective clinical study, Chin. J. Integr. Med. 23 (2016) 648–653, https://doi.org/10.1007/s11655-016-2581-3.
[13] S. Zhang, L. Shi, D. Mao, W. Peng, C. Sheng, C. Ding, F. Lin, C. Lei, S. Zhang, Use of Jianpi Jiedu herbs in patients with advanced colorectal cancer: a systematic review and meta-analysis, evidence-based complement, Alternative Med. 2018 (2018) 6180810, https://doi.org/10.1155/2018/6180810.
[14] W. Peng, S. Zhang, Z. Zhang, P. Xu, D. Mao, S. Huang, B. Chen, C. Zhang, S. Zhang, Jianpi Jiedu decoction, a traditional Chinese medicine formula, inhibits tumorigenesis, metastasis, and angiogenesis through the mTOR/HIF-1α/VEGF pathway, J. Ethnopharmacol. 224 (2018) 140–148, https://doi.org/10.1016/j.jep.2018.05.039.
[15] Chiu, The role of protein kinase C in the synergistic interaction of safingol and irinotecan in colon cancer cells, Int. J. Oncol. 35 (2009), https://doi.org/10.3892/ijo_00000465.
[16] D. Waghray, Q. Zhang, Inhibit or evade multidrug resistance P-glycoprotein in cancer treatment, J. Med. Chem. 61 (2017) 5108–5121, https://doi.org/10.1021/acs.jmedchem.7b01457.
[17] Y. Zhang, Z. Zeng, J. Zhao, D. Li, M. Liu, X. Wang, Measurement of rhodamine 123 in three-dimensional organoids: a novel model for P-glycoprotein inhibitor screening, Basic Clin. Pharmacol. Toxicol. 119 (2016) 349–352, https://doi.org/10.1111/bcpt.12596.
[18] H. Sato, M. Tamba, T. Ishii, S. Bannai, Cloning and expression of a plasma membrane cystine/glutamate exchange transporter composed of two distinct proteins, J. Biol. Chem. 274 (1999) 11455–11458, https://doi.org/10.1074/jbc.274.17.11455.
[19] X. Liu, M. Li, X. Wang, Z. Dang, L. Yu, X. Wang, Y. Jiang, Z. Yang, Effects of adjuvant traditional Chinese medicine therapy on long-term survival in patients with hepatocellular carcinoma, Phytomedicine 62 (2019) 152930, https://doi.org/10.1016/j.phymed.2019.152930.
[20] S. Huang, W. Peng, D. Mao, S. Zhang, P. Xu, P. Yi, S. Zhang, Kangai injection, a traditional Chinese medicine, improves efficacy and reduces toxicity of chemotherapy in advanced colorectal cancer patients: a systematic review and meta-analysis, evidence-based complement, Alternative Med. 2019 (2019) 8423037, https://doi.org/10.1155/2019/8423037.
[21] W. Wong, B.Z. Chen, A.K.Y. Lee, A.H.C. Chan, J.C.Y. Wu, Z. Lin, Chinese herbal medicine effectively prolongs the overall survival of pancreatic cancer patients: a case series, Integr. Cancer Ther. 18 (2019) 153473541982883, https://doi.org/10.1177/1534735419828836.
[22] M. Shakibaei, P. Kraehe, B. Popper, P. Shayan, A. Goel, C. Buhrmann, Curcumin potentiates antitumor activity of 5-fluorouracil in a 3D alginate tumor microenvironment of colorectal cancer, BMC Cancer 15 (2015) 250, https://doi.org/10.1186/s12885-015-1291-0.
[23] L. Shang, Y. Wang, J. Li, F. Zhou, K. Xiao, Y. Liu, M. Zhang, S. Wang, S. Yang, Mechanism of Sijunzi Decoction in the treatment of colorectal cancer based on network pharmacology and experimental validation, J. Ethnopharmacol. 302 (2023) 115876, https://doi.org/10.1016/j.jep.2022.115876.
[24] R. Li, J. Zhou, X. Wu, H. Li, Y. Pu, N. Liu, Z. Han, L. Zhou, Y. Wang, H. Zhu, L. Yang, Q. Li, Q. Ji, Jianpi Jiedu Recipe inhibits colorectal cancer liver metastasis via regulating ITGBL1-rich extracellular vesicles mediated activation of cancer-associated fibroblasts, Phytomedicine 100 (2022) 154082, https://doi.org/10.1016/j.phymed.2022.154082.
[25] T. Wang, J. Liu, X. Luo, L. Hu, H. Lu, Functional metabolomics innovates therapeutic discovery of traditional Chinese medicine derived functional compounds, Pharmacol. Ther. 224 (2021) 107824, https://doi.org/10.1016/j.pharmthera.2021.107824.
[26] X. Jiang, B.R. Stockwell, M. Conrad, Ferroptosis: mechanisms, biology and role in disease, Nat. Rev. Mol. Cell Biol. 22 (2021) 266–282, https://doi.org/10.1038/s41580-020-00324-8.
[27] C. Zhang, X. Liu, S. Jin, Y. Chen, R. Guo, Ferroptosis in cancer therapy: a novel approach to reversing drug resistance, Mol. Cancer 21 (2022) 47, https://doi.org/10.1186/s12943-022-01530-y.
[28] H. Zhang, T. Deng, R. Liu, T. Ning, H. Yang, D. Liu, Q. Zhang, D. Lin, S. Ge, M. Bai, X. Wang, L. Zhang, H. Li, Y. Yang, Z. Ji, H. Wang, G. Ying, Y. Ba, CAF secreted miR-522 suppresses ferroptosis and promotes acquired chemo-resistance in gastric cancer, Mol. Cancer 19 (2020) 43, https://doi.org/10.1186/s12943-020-01168-8.
[29] C. Yang, Y. Zhang, S. Lin, Y. Liu, W. Li, Suppressing the KIF20A/NUAK1/Nrf2/GPX4 signaling pathway induces ferroptosis and enhances the sensitivity of colorectal cancer to oxaliplatin, Aging 13 (2021) 13515–13534, https://doi.org/10.18632/aging.202774.
[30] P. Koppula, L. Zhuang, B. Gan, Cystine transporter SLC7A11/xCT in cancer: ferroptosis, nutrient dependency, and cancer therapy, Protein Cell 12 (2020) 599–620, https://doi.org/10.1007/s13238-020-00789-5.
[31] D. Fu, C. Wang, L. Yu, R. Yu, Induction of ferroptosis by ATF3 elevation alleviates cisplatin resistance in gastric cancer by restraining Nrf2/Keap1/xCT signaling, Cell. Mol. Biol. Lett. 26 (2021) 26, https://doi.org/10.1186/s11658-021-00271-y.